frontiers | Frontiers in Immunology

TYPE Original Research
PUBLISHED 11 November 2022
DOI 10.3389/fimmu.2022.1022093

OPEN ACCESS

EDITED BY
Eun Jeong Park,
Mie University, Japan

REVIEWED BY
Sunita Keshari,
University of Texas MD Anderson Cancer Center, United States
Wei Li,
Fudan University, China

*CORRESPONDENCE
Xiaolong A. Zhou
alan.zhou@northwestern.edu

†These authors share first authorship

‡These authors share senior authorship

SPECIALTY SECTION
This article was submitted to Molecular Innate Immunity, a section of the journal Frontiers in Immunology

RECEIVED 18 August 2022
ACCEPTED 19 October 2022
PUBLISHED 11 November 2022

CITATION
Hooper MJ, Enriquez GL, Veon FL, LeWitt TM, Sweeney D, Green SJ, Seed PC, Choi J, Guitart J, Burns MB and Zhou XA (2022) Narrowband ultraviolet B response in cutaneous T-cell lymphoma is characterized by increased bacterial diversity and reduced *Staphylococcus aureus* and *Staphylococcus lugdunensis*. *Front. Immunol.* 13:1022093. doi: 10.3389/fimmu.2022.1022093

Narrowband ultraviolet B response in cutaneous T-cell lymphoma is characterized by increased bacterial diversity and reduced *Staphylococcus aureus* and *Staphylococcus lugdunensis*

Madeline J. Hooper[1†], Gail L. Enriquez[2†], Francesca L. Veon[1], Tessa M. LeWitt[1], Dagmar Sweeney[3], Stefan J. Green[4], Patrick C. Seed[5], Jaehyuk Choi[1], Joan Guitart[1], Michael B. Burns[2‡] and Xiaolong A. Zhou[1*‡]

[1]Department of Dermatology, Northwestern University, Feinberg School of Medicine, Chicago, IL, United States, [2]Department of Biology, Loyola University Chicago, Chicago, IL, United States, [3]Genome Research Core, University of Illinois at Chicago, Chicago, IL, United States, [4]Genomics and Microbiome Core Facility, Rush University Medical Center, Chicago, IL, United States, [5]Division of Pediatric Infectious Diseases, Ann & Robert H. Lurie Children's Hospital of Chicago, Chicago, IL, United States

Skin microbiota have been linked to disease activity in cutaneous T-cell lymphoma (CTCL). As the skin microbiome has been shown to change after exposure to narrowband ultraviolet B (nbUVB) phototherapy, a common treatment modality used for CTCL, we performed a longitudinal analysis of the skin microbiome in CTCL patients treated with nbUVB. 16S V4 rRNA gene amplicon sequencing for genus-level taxonomic resolution, *tuf2* amplicon next generation sequencing for staphylococcal speciation, and bioinformatics were performed on DNA extracted from skin swabs taken from lesional and non-lesional skin of 25 CTCL patients receiving nbUVB and 15 CTCL patients not receiving nbUVB from the same geographical region. Disease responsiveness to nbUVB was determined using the modified Severity Weighted Assessment Tool: 14 (56%) patients responded to nbUVB while 11 (44%) patients had progressive disease. Microbial α-diversity increased in nbUVB-responders after phototherapy. The relative abundance of *Staphylococcus*, *Corynebacterium*, *Acinetobacter*, *Streptococcus*, and *Anaerococcus* differentiated nbUVB responders and non-responders after treatment ($q<0.05$). Microbial signatures of nbUVB-treated patients demonstrated significant post-exposure depletion of *S. aureus* ($q=0.024$) and *S. lugdunensis* ($q=0.004$) relative abundances. Before nbUVB, responder lesional skin harboured higher levels of *S. capitis* ($q=0.028$) and *S. warneri* ($q=0.026$) than non-responder lesional skin. *S. capitis* relative abundance increased in the lesional skin of responders ($q=0.05$) after phototherapy; a similar upward trend was observed in non-responders ($q=0.09$). Post-

treatment skin of responders exhibited significantly reduced *S. aureus* (q=0.008) and significantly increased *S. hominis* (q=0.006), *S. pettenkoferi* (q=0.021), and *S. warneri* (q=0.029) relative abundances compared to that of no-nbUVB patients. *Staphylococcus* species abundance was more similar between non-responders and no-nbUVB patients than between responders and no-nbUVB patients. In sum, the skin microbiome of CTCL patients who respond to nbUVB is different from that of non-responders and untreated patients, and is characterized by shifts in *S. aureus* and *S. lugdunensis*. Non-responsiveness to phototherapy may reflect more aggressive disease at baseline.

KEYWORDS

cutaneous T-cell lymphoma, microbiome, phototherapy, cancer, oncology, dermatology

Introduction

Cutaneous T-cell lymphoma (CTCL) is a rare non-Hodgkin's lymphoma in which malignant T-cells infiltrate the skin. Although the etiology of CTCL remains unexplained, bacteria inhabiting the skin are understood to drive disease flares and the pathophysiology therein – specifically, *S. aureus* enterotoxin and alpha-toxin are tied to pronounced oncogenesis in CTCL (1–4). Additionally, CTCL patients have an increased risk of skin infections compared to the general population and such infections tend to be associated with disease progression (5). Influenced by local physiochemical properties and adjacent physical, autoimmune, and infectious trauma, the skin comprises a site-specific microbial niche rich with therapeutic and prognostic utility in cutaneous disease (6–8). Commensal skin bacteria play important roles in immune education and skin barrier homeostasis, and with dysbiosis comes disruption of these essential mechanisms (9). Mirroring this observation, specific changes in the skin microbiome have been associated with immune-mediated inflammatory skin conditions, including atopic dermatitis (AD) (10, 11), psoriasis (12, 13), hidradenitis suppurativa (14, 15), and vitiligo (16, 17). Nasal and gut dysbiosis have also been linked to these same diseases (15, 18). Considering recent research demonstrating CTCL patients harbor altered nasal and gut microbiota, and data revealing distinct bacterial communities distinguish healthy from lesional skin, CTCL may be a disease of global dysbiosis (19–25). While direct causality between dysbiosis and disease progression remains to be demonstrated, these findings are highly anticipated as they may precipitate innovative management strategies for CTCL patients.

Narrowband ultraviolet B (nbUVB) phototherapy is a common treatment modality for CTCL with an overall response rate of 89% in early-stage disease (26). Notably effective for skin-limited CTCL, nbUVB has been shown to shape the skin microbiome in association with disease improvement in AD and vitiligo (10, 11, 16). Interestingly, nbUVB in AD was observed to decrease lesional skin *Staphylococcus* abundance, induce clinical improvement, and enhance the anti-*S. aureus* activity and treatment effects of topical corticosteroids (11). *In vitro* studies have demonstrated ultraviolet light can suppress *S. aureus* superantigen production (27). Furthermore, excimer laser-mediated increases of *Cyanobacterium* in AD skin may reflect improved skin water content (10), thereby supporting the hypothesis that non-*Staphylococcus* taxa also play an important role in the homeostasis of skin health and disease.

We conducted a longitudinal study of the bacterial communities populating the lesional and non-lesional skin of CTCL patients treated with nbUVB phototherapy. This early effort to detail a therapeutic-microbial relationship in CTCL achieves two aims: first, to assess the impact of nbUVB on the CTCL skin microbiome; and second, to provide a comprehensive framework for evaluating the biological relevance of the microbial differences separating healthy and diseased skin.

Materials and methods

Participants

Ethical approval was obtained from the Northwestern University Institutional Review Board (STU00209226). In compliance with the Declaration of Helsinki, 40 patients with clinically- and biopsy-confirmed CTCL, as reviewed by an expert dermatopathologist (JG), were consented and enrolled in the study between 2019 and 2021. Specimen and data collection were performed at the Northwestern University Cutaneous Lymphoma specialty clinic. Clinical staging and modified

Severity Weighted Assessment Tool (mSWAT) were assessed by the principal investigator (XAZ) at sample collection.

Figure 1 illustrates the study design. Twenty-five patients were prescribed a treatment regimen involving nbUVB phototherapy; the remaining 15 participants used non-nbUVB standard-of-care treatments. In total, 28 patients used topical treatments, of which 89% (n=25) were using topical corticosteroid monotherapy, 14 patients used systemic treatments, and 8 were treatment naïve. The great majority of patients (85%) had been stable on these therapies for minimum 24 months prior to study enrollment. Patients who used antibiotics in the 4 weeks prior to sample collection were excluded.

16S rRNA amplification and sequencing

Genomic DNA was prepared for sequencing using a two-stage amplicon sequencing workflow, as described previously (28). Genomic DNA was PCR-amplified using primers targeting the V4 region of microbial 16S rRNA genes. The primers, 515F modified and 806R modified, contained 5' linker sequences compatible with Access Array primers for Illumina sequencers (Fluidigm; South San Francisco, CA) (29). PCRs were performed in a total volume of 10µL using MyTaq^{TM} HS 2X Mix (Bioline; Memphis, TN), primers at 500nM concentration, and approximately 1,000 copies per reaction of a synthetic double-stranded DNA template (described below). Thermocycling conditions were 95°C for 5' (initial denaturation), followed by 28 cycles of 95°C for 30 sec, 55°C for 45 sec, and 72°C for 30 sec. The second-stage PCR reaction contained 1µL of PCR product from each reaction and a unique primer pair of Access Array primers. Thermocycling conditions were 95°C for 5' (initial denaturation), followed by 8 cycles of 95°C for 30 sec, 60°C for 30 sec, and 72°C for 30 sec. Libraries were pooled and sequenced on an Illumina MiniSeq sequencer (Illumina; San Diego, CA) with 15% phiX spike-in and paired-end 2x153 base sequencing reads.

A synthetic double-stranded DNA spike-in was created as a gBLOCK by Integrated DNA Technologies (IDT; Coralville, IA). The design basis was a 999 base pair (bp) region of the 16S rRNA gene of *Rhodanobacter denitrificans* strain 2APBS1^{T} (NC_020541) (30). Portions of V1, V2, and V4 variable regions were replaced by eukaryotic mRNA sequences (*Apostichopus japonicus* glyceraldehyde-3-phosphate dehydrogenase mRNA, HQ292612 and *Strongylocentrotus intermedius* glyceraldehyde-3-phosphate dehydrogenase mRNA, KC775387). Primer sites were preserved, and the overall length of the synthetic DNA did not differ from the equivalent *R. denitrificans* fragment. PCR amplicons generated from this synthetic DNA do not differ in size from bacterial amplicons and can only be identified and removed through post-sequencing bioinformatics analysis. The sequence can be accessed *via* GenBank (OK324963).

Basic processing

Sequencing resulted in a total of 23,825,736 reads with an average of 42,698 reads per sample. Forward (F) and reverse (R)

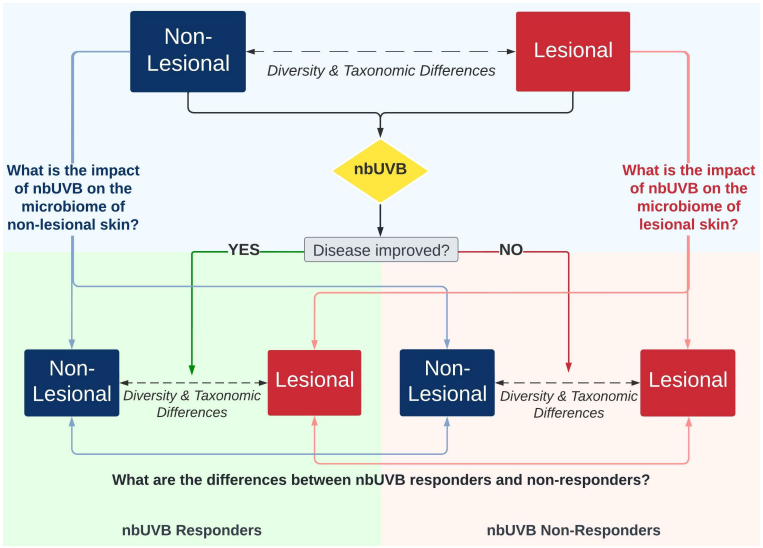

FIGURE 1
Investigational schemata for evaluating the skin microbiome of lesional and non-lesional cutaneous T-cell lymphoma (CTCL) skin in response to narrowband ultraviolet B (nbUVB) phototherapy. Differences in microbial community diversity and taxonomic abundance between responders and non-responders are illustrated in Figures 2–5.

reads were trimmed using cutadapt v3.5 to remove primer sequences (31). All reads were trimmed and filtered based on quality using the default parameters within dada2 v1.22 (32) with the following modification: the truncLen parameter was disabled, and maxEE for all reads was set to 1,1. The error models were initiated using $5x10^8$ randomized bases for the F and R sets. Following subsequent denoising with dada2's divisive partitioning machine learning approach, F and R amplicon sequence variant (ASV) read pairs were merged with a maxMismatch of 0 and a minOverlap of 8 bases. Merged pairs that did not fall within the expected length window of 252-254 bases were removed. Chimeric sequences were identified and removed using a *de novo* approach within dada2 assessing the entire sequence pool as a whole. ASVs were assigned taxonomy using DECIPHER v2.22 with the SILVA v138 training set (33, 34). The synthetic spike-in sequences were then removed from the dataset. The decontam R package v1.14 was used to identify potentially contaminating sequences, using environmental control samples collected at experimental sample collection (35). Suspected contaminant ASVs above the default prevalence threshold of 0.1 were classified as potential environmental artifacts and removed from the dataset. An abundance filter of 0.1% and a prevalence filter of 10% were applied. Following QC processing, decontamination, and filtering, there were a total of 5,862,546 merged read pairs with an average of 17,042 per sample. To maximize data retention, while removing uninformative patient samples, only samples with minimum 1000 reads following processing were retained. Patient samples were paired across disease status (lesional, non-lesional) and time (pre-nbUVB, post-nbUVB). Only complete patient-matched sets were retained for analysis.

Tuf2 amplicon next generation sequencing

Genomic DNA was PCR amplified with primers CS1_tuf2-F (ACACTGACGACATGGTTCTACAACAGGCCGTGTTGAACGTG) and CS2_tuf2-R (TACGGTAGCAGAGACTTGGTCTACAGTACGTCCACCTTCACG) (36, 37) targeting the *Staphylococcus tuf* gene. Amplicons were generated using a two-stage PCR amplification protocol, as previously described (28). First stage PCR amplifications were performed in 10µL reactions in 96-well plates, using MyTaq HS 2X mastermix (Bioline). PCR conditions were 95°C for 5 min, followed by 28 cycles of 95°C for 30 sec, 55°C for 30 sec and 72°C for 60 sec. Second-stage reactions using Access Array primers were performed as described above. Samples were pooled, purified, and sequenced on an Illumina MiSeq with 10% phiX spike-in and paired-end 2x300 base sequencing reads (*i.e.*, V3 chemistry). Library preparation, pooling, and sequencing were performed at the Genome Research Core within the Research Resources Center at the University of Illinois at Chicago.

Tuf2 amplicon processing

Tuf2 sequencing generated a total of 27,022,394 reads with an average of 57,372 raw reads per sample. Primer trimming and denoising were accomplished using the same procedure as above for the 16S amplicon data with the following modifications: during filtering and trimming, the maxEE for all reads was set to 3,3 due to their increased length, read merging used default parameters, and the read length cutoff window range was 400-500 nucleotides for merged read pairs. Following processing there were a total of 4,496,566 reads retained for an average sample read count of 9,547. ASVs were taxonomically annotated using BLASTn alignments against NCBI prokaryotic (nr) refseq database (online access 14 June 2022). Only taxa that were within the *Staphylococcus* genus were retained.

Statistical analyses

The samples in the cleaned ASV table were visually evaluated using phyloseq v1.38 (38). α-diversity metrics were generated using the ASV table rarefied to 1000 sequences. Differences in α-diversity (Observed OTUs, Chao1, Shannon, and Simpson indices) between patient sets were calculated using Wilcoxon rank-sum non-paired tests from the stats R package (39) while differences within patient-matched samples were calculated using Pairwise Wilcoxon rank-sum tests. β-diversity metrics were generated using the rarefied ASV table. Principal coordinate analysis (PCoA) with Bray-Curtis dissimilarity was performed to identify β-diversity using an ADONIS2 method (permutations = 500) of vegan v2.5.7 (40). To verify the PCoA findings, "createDataPartition" function from the Caret package v6.0.93 was used to split the data into training and test sets (41) and a supervised machine-learning algorithm Random Forest from the random Forest package v 4.7.1.1 was applied for a 10-fold cross-validation in R. The model was created using 1500 trees (42). To evaluate the model, receiver operating characteristic curves and area under the curve (AUC) values were generated using the "roc" function of the R pROC package v1.18.0 (43). Differential abundance analysis was conducted by metagenomeSeq v1.36 (44) using the non-rarefied ASV table, with ASVs removed if they had less than 4 counts or a prevalence below 10% across the sample set. A zero-inflated Gaussian (ZIG) log-normal model was implemented using the "fitFeatureModel" function of the metagenomeSeq R package to compare abundance of taxa among different groups. To further refine the differential taxa results and to reduce the likelihood of false positives, a second method, edgeR v3.36 (45), was applied to the same ASV table. For both the metagenomeSeq and edgeR results, significant ASVs were only considered if they achieved a false discovery rate (FDR)-adjusted p-value of <0.05 (q-value) by both methods.

The post-process *tuf2* ASV and taxa table was filtered using phyloseq v1.38 (38). To identify the most abundant *Staphylococcus* species, filters of minimum 20% prevalence and

4 ASVs were applied. After centered log-ratio (CLR) transformation, the final ASV table including only the *Staphylococcus* species present at 20% abundance or greater was used for statistical analysis. Differences in abundance between patient groups were calculated using Wilcoxon rank-sum non-paired tests from the stats R package (39) while Pairwise Wilcoxon rank-sum tests were used to calculate differences between patient-matched samples. Differential abundance analysis was conducted using the CLR transformed abundance table. A ZIG log-normal model as described above was implemented to compare abundance of the top 8 *Staphylococcus* species among different groups. Significant ASVs were only considered if they achieved a FDR of <0.05.

Results

Patient characteristics

Table 1 summarizes patient characteristics. Of the 25 CTCL patients treated with nbUVB, 20 were diagnosed with mycosis fungoides, 2 with Sézary syndrome, and 3 with other CTCL subtypes. The patients were predominately male (n=17, 68.0%) and Caucasian (n=19, 76.0%). Fifteen sex-, age-, and race-matched patients who were not treated with nbUVB phototherapy (NT) were also included (Table 2). On average, nbUVB-treated participants were evaluated after 6.2 months (range 1.6-14.7) of treatment, at which time 14 patients (56.0%) had improved disease (Responders [R]; mean mSWAT change -18.5) and 11 (44.0%) had progressive disease (Non-Responders [NR]; mean mSWAT change +11.4). There were no significant differences in demographic or clinical characteristics between R and NR (p>0.05).

Treated patients were prescribed nbUVB two or three times per week. All patients endorsed using standard-of-care topical (n=31) and systemic (n=14) CTCL treatments (Supplemental Table S1). Hypercholesterolemia (n=21) and hypertension (n=17) were the most common comorbidities across the entire cohort. There were no significant differences in treatment profiles or comorbidity prevalence amongst R, NR, and NT groups (p=0.822 and p=0.656, respectively).

TABLE 1 Patient demographic and clinical characteristics.

	Responders	Non-responders	*p-value*
N	14	11	
Mean age (range), years[†]	58 (35-78)	57 (36-72)	0.857
Sex (%)[‡]			1.000
Male	10 (71.4)	7 (63.6)	
Female	4 (28.6)	4 (36.4)	
Race (%)[‡]			0.333
White	11 (78.6)	8 (72.7)	
African American	1 (7.1)	3 (27.3)	
Other	2 (14.3)	0 (0.0)	
FST (%)[‡]			0.623
Light (I-III)	12 (85.7)	8 (72.7)	
Dark (IV-VI)	2 (14.3)	3 (27.3)	
CTCL Subtype (%)[‡]			0.774
Mycosis fungoides	12 (85.7)	8 (72.7)	
Sézary syndrome	1 (7.1)	1 (9.1)	
Other CTCL	1 (7.1)	2 (18.2)	
Stage (%)[‡]			0.115
Early (IA-IIA)	11 (78.6)	5 (45.5)	
Late (IIB-IVB)	3 (21.4)	6 (54.5)	
Non-nbUVB treatments (%)[‡]			0.927
Skin-directed only	7 (50.0)	4 (36.4)	
Systemic only	1 (7.1)	1 (0.1)	
Skin-directed and systemic	3 (21.4)	4 (36.5)	
None	3 (21.4)	2 (18.2)	
Mean change in mSWAT, pre- versus post-nbUVB (range)	-18.5 (-52 - -1)	11.4 (2-79)	0.002[†]

CTCL, cutaneous T-cell lymphoma; FST, Fitzpatrick skin phototype; mSWAT, modified Severity Weighted Assessment Tool; nbUVB, narrowband ultraviolet B.
[†]Independent T-test, [‡]Fisher exact test.

TABLE 2 Demographic and clinical characteristics of patients not treated with nbUVB (NT) compared to nbUVB responders (R) and non-responders (NR).

	No nbUVB (NT)	R vs NT, *p-value*	NR vs NT, *p-value*
N	15		
Mean age (range), years[†]	64 (37-83)	0.307	0.188
Sex (%)[‡]		1.000	1.000
Male	10 (66.7)		
Female	5 (33.3)		
Race (%)[‡]		0.791	0.279
White	13 (86.7)		
African American	0 (0.0)		
Other	2 (13.3)		
FST (%)[‡]		0.598	0.279
Light (I-III)	14 (93.3)		
Dark (IV-VI)	1 (6.7)		
CTCL Subtype (%)[‡]		1.000	1.000
Mycosis fungoides	11 (73.4)		
Sézary syndrome	2 (13.3)		
Other CTCL	2 (13.3)		
Stage (%)[‡]		0.009	0.419
Early (IA-IIA)	4 (26.6)		
Late (IIB-IVB)	11 (73.4)		
Treatments (%)[‡]		0.884	0.925
Skin-directed only	7 (46.7)		
Systemic only	0 (0.0)		
Skin-directed and systemic	5 (33.3)		
None	3 (20.0)		
Mean change in mSWAT, pre- versus post-nbUVB (range)[†]	3.2 (-10 - 37)	0.807	

CTCL, cutaneous T-cell lymphoma; FST, Fitzpatrick skin phototype; mSWAT, modified Severity Weighted Assessment Tool; nbUVB,narrowband ultraviolet B.
[†]Independent T-test, [‡]Fisher exact test.

Biodiversity and community richness modulated by nbUVB

The pre-nbUVB microbial communities of R and NR were distinct in both lesional (Bray-Curtis index; $R^2 = 0.049$, p=0.012; AUC=0.852) and non-lesional skin ($R^2 = 0.077$, p=0.004; AUC=0.796) (Figure 2A). After phototherapy, R and NR non-lesional microbiota remained distinct ($R^2 = 0.030$, p=0.045; AUC=0.852), but lesional communities became non-distinct ($R^2 = 0.031$, p=0.089; AUC=0.759) (Figure 2B). As expected, the PCoA plots show between-group overlap because the samples are all from the same microbial niche.

Phylogenetic diversity increased in all treated patients' skin after phototherapy (observed p=0.009; Chao1 p=0.016) (Figure 2C). Post-nbUVB, lesional α-diversity was significantly greater in R than in NR (Shannon p=0.0024; Simpson p=0.0093) (Figure 2D). This difference corresponded to a significant increase in α-diversity after nbUVB in R skin (lesional: observed p=0.007, Chao1 p=0.002; non-lesional: observed p=0.001, Chao1 p=0.002) (Figures 2E, F) while no significant changes were noted in NR skin (lesional: observed p=0.160, Chao1 p=0.260; non-lesional: observed p=0.640, Chao1 p=0.330) (Figures 2G, H).

Decreased *Staphylococcus*, increased *Acinetobacter* differentiate nbUVB responsiveness after phototherapy

The genera *Staphylococcus*, *Corynebacterium*, and *Acinetobacter* predominated all analyzed specimens (Figure 3A). Differential analyses revealed significant genus-level shifts that distinguished R and NR, and lesional and non-lesional skin in response to phototherapy (q<0.05). In addition to genus-level taxonomic shifts, several specific ASVs within these genera provided opposing abundance shifts across the patient sample set. Figure 4 summarizes these genus-level taxon-by-taxon differences with specific reference to the unique ASV shifts, as appropriate.

10.3389/fimmu.2022.1022093

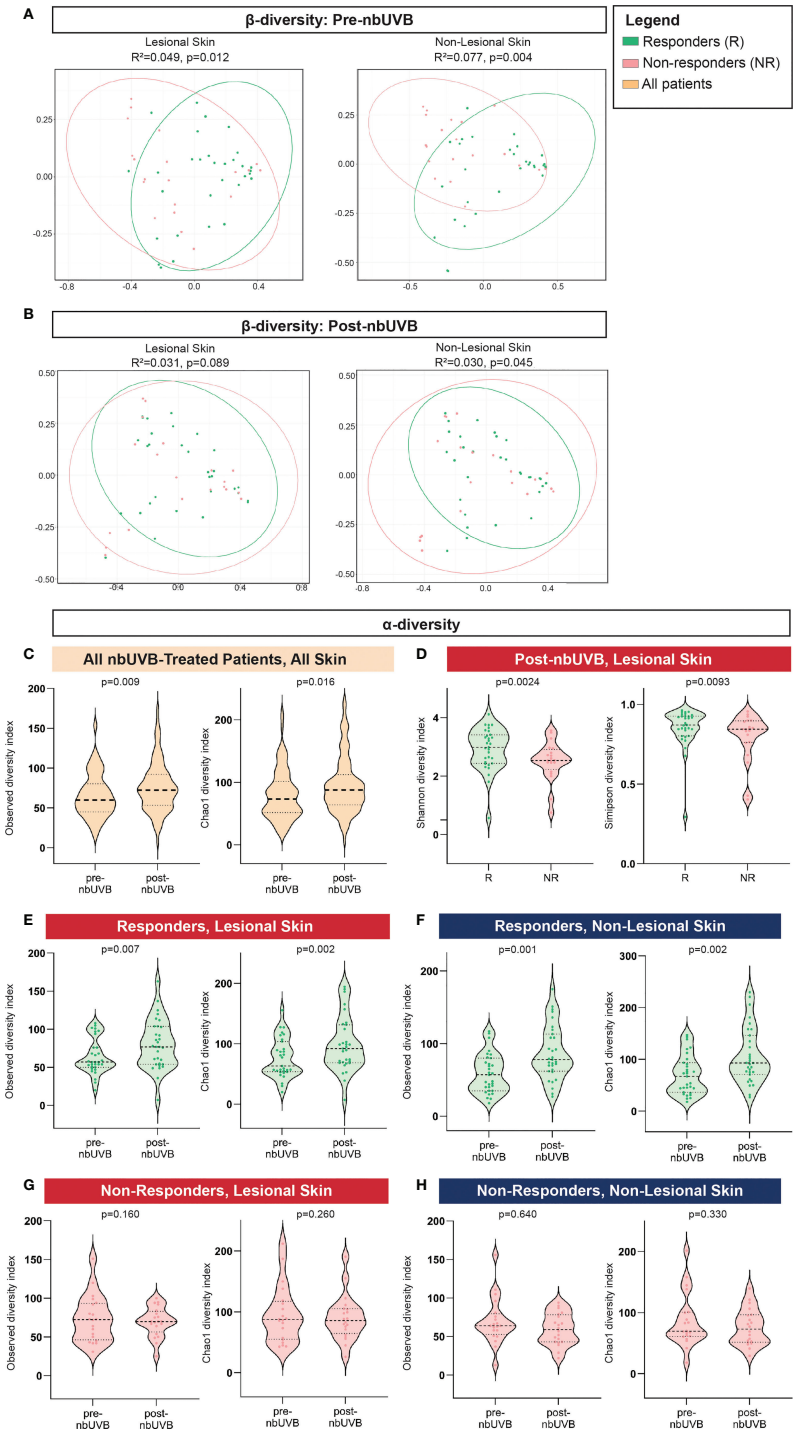

FIGURE 2
Distinct microbial communities comprise the skin microbiota of nbUVB responders and non-responders before and after nbUVB. **(A)** Bray-Curtis dissimilarity indices demonstrated Responder (R) and Non-Responder (NR) bacterial skin communities were distinct prior to nbUVB in lesional and non-lesional skin. **(B)** R versus NR post-nbUVB community differences approached significance in lesional skin, but reached significance in non-lesional skin. **(C)** Amongst all nbUVB-treated patients, α-diversity increased after phototherapy. **(D)** Following nbUVB, α-diversity of lesional skin was higher in R than NR. **(E)** α-diversity of R lesional skin and **(F)** non-lesional skin significantly increased after phototherapy. **(G)** No pre- versus post-nbUVB α-diversity differences were noted in NR lesional or **(H)** non-lesional skin. Thick dashed horizontal black lines indicate group median; thin dashed lines indicate 1st and 3rd quartiles.

10.3389/fimmu.2022.1022093

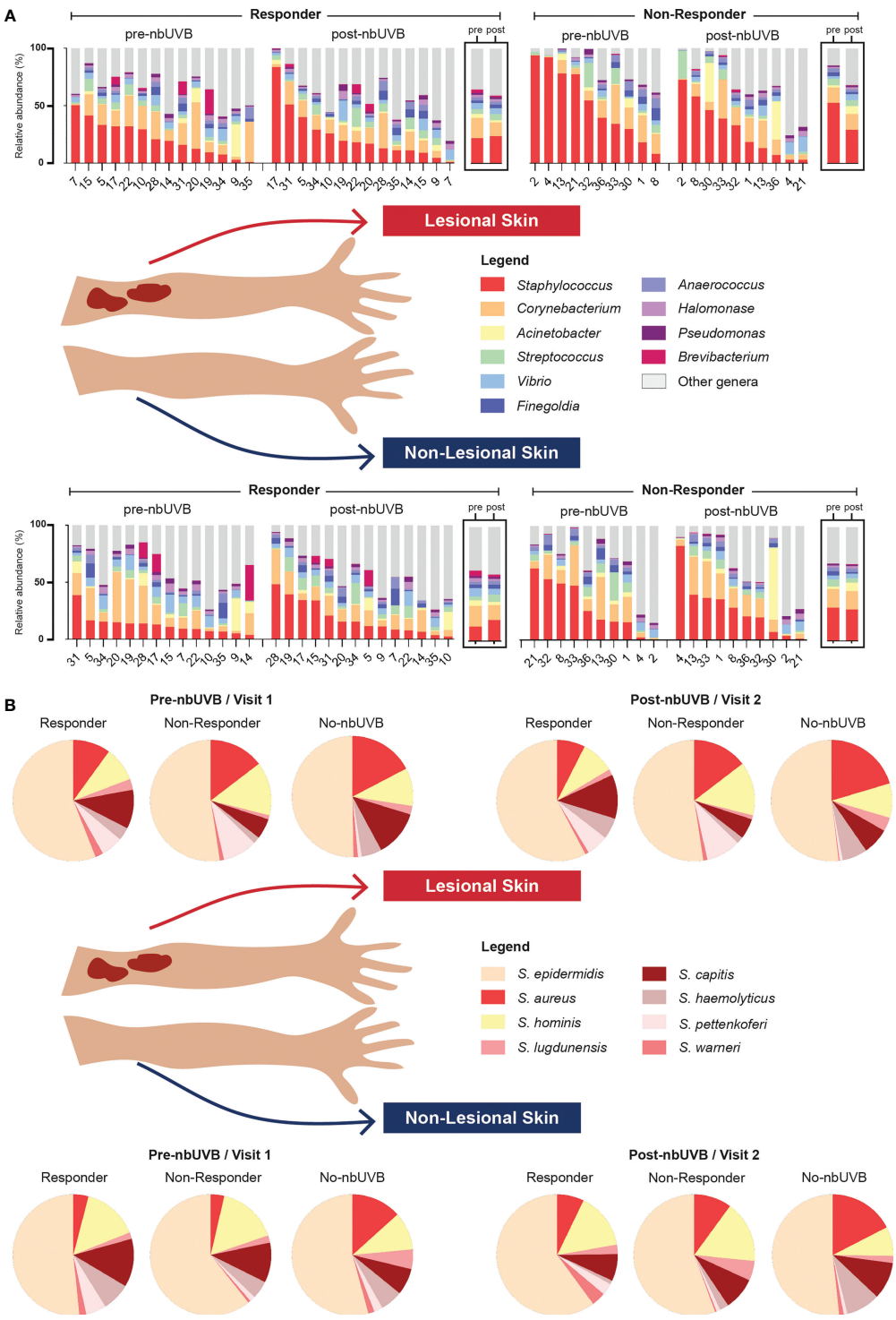

FIGURE 3
Microbial communities of CTCL lesional and non-lesional skin are predominated by different taxa. **(A)** At the taxonomic level of genus, *Staphylococcus*, *Corynebacterium*, and *Acinetobacter* were the most prevalent and abundant genera present in all treated samples. Bar charts indicate relative abundance (%) of the 10 most abundant genera populating the skin of each patient; boxed graphs reflect group mean relative abundance at pre-nbUVB (left) and post-nbUVB (right). Subject IDs are indicated along the x-axis and ordered to best visualize the distribution of relative abundances in descending order. Of note, this figure is not intended to illustrate statistically significant differences. **(B)** Staphylococcal speciation across all samples revealed a majority presence of *S. epidermidis*, *S. aureus*, and *S. hominis*. Pie charts reflect mean relative abundance of each species identified across R, NR, and no-nbUVB patient groups.

10.3389/fimmu.2022.1022093

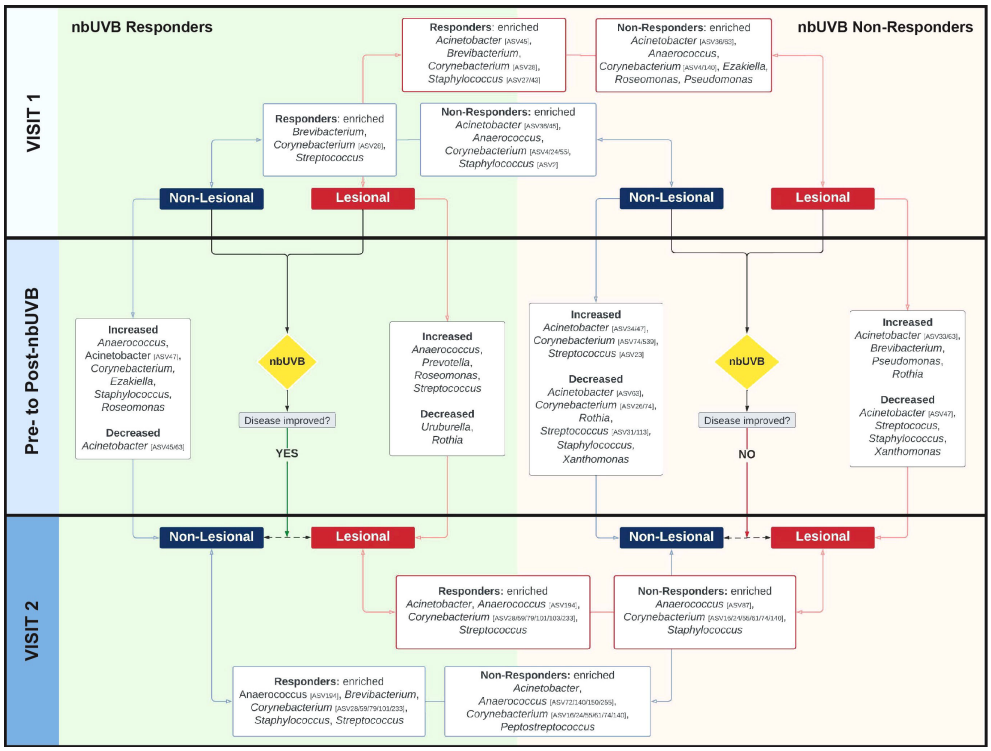

FIGURE 4
The skin microbiome changes after exposure to nbUVB phototherapy, as demonstrated by shifts at the taxonomic level of genus. Map of genus-level taxa abundances differentiating responders (R) and non-responders (NR) at lesional and non-lesional sites. Panels represent specific analyses: pre-nbUVB (top panel), pre- versus post-nbUVB (middle panel), and post-nbUVB (bottom panel). In cases of mixed responses at the genus level, specific ASVs identified on differential analysis are noted. Bidirectional arrows indicate the skin sites being compared at the same time point (e.g., R/lesional skin/pre-nbUVB versus NR/lesional skin/pre-nbUVB); unidirectional arrows indicate longitudinal shifts (e.g., R/lesional skin/pre-nbUVB versus R/lesional skin/post-nbUVB).

Pre-nbUVB treatment

Before phototherapy, *Brevibacterium*, *Staphylococcus* ASV27, and *Staphylococcus* ASV43 were significantly more abundant in eventual R relative to eventual NR across both lesional and non-lesional sites. Comparing non-lesional samples, *Streptococcus* was more abundant in R and *Staphylococcus* ASV2 was more abundant in NR. Mixed responses among several *Corynebacterium* ASVs were observed: ASV28 was more abundant in R, while ASV4 was more abundant in NR. At lesional sites, *Acinetobacter* ASV45 was greater in R than NR while *Acinetobacter* ASV36 was depleted in R; at non-lesional sites, both *Acinetobacter* ASV45 and ASV36 were more abundant in R.

Comparing pre- and post-nbUVB treatment

Pre- versus post-phototherapy comparisons of R lesional skin showed increased abundance of *Streptococcus*, *Anaerococcus*, and *Prevotella* after nbUVB treatment (Figure 4). In contrast, NR lesional skin demonstrated a reduction of *Streptococcus*, *Staphylococcus*, and *Acinetobacter*. R and NR shared some non-lesional genus-level similarities: mixed changes were observed amongst *Acinetobacter* ASVs (decreased ASV63; increased ASV47) and several *Corynebacterium* ASVs were more abundant (ASV16/233 in R, ASV74/539 in NR). While R patient samples revealed increased relative abundance of lesional *Streptococcus* ASV31, NR lesional skin exhibited a loss of this ASV.

Post-nbUVB treatment

Finally, post-nbUVB R lesional skin was differentiated from NR lesional skin by greater relative abundance of *Acinetobacter* and *Streptococcus*, and lower relative abundance of *Staphylococcus*. A mixed abundance distribution across several *Corynebacterium* ASVs was observed in R compared to NR skin: increased ASV101/103/233/28/59/79, and decreased ASV140/16/24/55/61/74. The pre-nbUVB differences in *Brevibacterium* and *Corynebacterium* identified between R and NR non-lesional skin persisted after nbUVB.

With ASVs collapsed by genus, taxon-by-taxon analysis revealed *Streptococcus* comprised a larger relative abundance in R than NR lesional skin (p=0.008, q=0.08) after phototherapy; this comparison approached significance in non-lesional skin (p=0.047, q=0.260). In the pre- versus post-nbUVB analysis, loss

of *Corynebacterium* across all lesional sites trended towards significance (p=0.033, q=0.330).

Genus-level differences distinguishing nbUVB-treated patients from no-nbUVB patients

No pre- versus post-nbUVB changes in NT α- or β-diversity were observed (Shannon p=0.51; Bray-Curtis R^2 = 0.007, p=0.425). Differential analysis of microbial profiles at the genus level between treated and NT patients revealed phototherapy has similar effects on the skin microbiota regardless of disease response. Comparison of R and NT at visit 2 demonstrated *Acinetobacter* and *Corynebacterium* (ASV24/55) were more abundant in NT, whereas *Corynebacterium* ASV233 and *Streptococcus* were more abundant in R. Similarly, NR versus NT analysis indicated *Acinetobacter* and *Corynebacterium* (ASV16) were more abundant in NT. *Peptostreptococcus* and *Anaerococcus* were more abundant in NR.

Shifts in *Staphylococcus* species abundance are associated with nbUVB responsiveness

Given the changes in relative abundance of *Staphylococcus* at the genus level and considering the importance of these species to skin health, we next assessed *Staphylococcus* species-level relative abundance within our samples using tuf amplicon sequencing. The most prevalent and abundant species were *S. epidermidis*, *S. aureus*, and *S. hominis* (Figure 3B).

Analysis of pre-nbUVB R versus NR revealed greater relative abundances of *S. capitis* (q=0.028) and *S. warneri* (q=0.026) characterized R lesional skin (Figure 5A). Pre-treatment non-lesional skin also exhibited greater relative abundance of *S. warneri* in R than NR (q=0.032), while *S. hominis* relative abundance trended higher in NR than R (q=0.084) (Figure 5A). Pre- versus post-nbUVB assessment demonstrated *S. capitis* communities were significantly more abundant in R lesional skin (q=0.05) and trended higher in NR lesional skin (q=0.09) after phototherapy (Figure 5B). Across all sites, relative abundance of *S. aureus* (q=0.024) and *S. lugdunensis* (q=0.004) significantly decreased after phototherapy in R while *S. warneri* increased in NR (q=0.032). Lastly, post-nbUVB *S. haemolyticus* relative abundance trended higher in R compared to NR lesional skin (q=0.081) (Figure 5C). Post-treatment R versus NT analysis revealed R skin was characterized by significantly less abundant *S. aureus* (q=0.008) and significantly more abundant *S. hominis* (q=0.006), *S. pettenkoferi* (q=0.021), and *S. warneri* (q=0.029). NR versus NT comparisons revealed *S. capitis* relative abundance was greater in NR (q=0.004) while *S. haemolyticus* was more abundant in NT (q=0.037).

Discussion

The antigenic stimulation provided by skin microbiota and bacterial toxins is likely one of several phenomena that, in concert with chronic skin inflammation, drives CTCL progression. Our observations suggest that successful treatment with phototherapy is associated with a microbial signature unique from that of untreated disease and phototherapy-refractory disease. This finding could suggest skin microbiota may play a role in nbUVB-responsiveness; conversely, improved disease may be characterized by a distinct microbial signature outside of any nbUVB-related effects. The increased α-diversity of nbUVB responders' skin also supports the hypothesis that phototherapy helps recoup microbial richness that may be lost in CTCL. This change could be explained by targeted attenuation of abundant taxa, such as *S. aureus* and *S. lugdunensis*, as seen in this dataset. Because the influence of cutaneous microbes on skin health is manifold, these findings underscore the potential role of commensal skin bacteria in CTCL pathogenesis and the therapeutic applications therein.

The current literature strongly supports a key role for *S. aureus* in CTCL progression (2, 3, 46); however, little is known about the influence of other staphylococcal species. We noted baseline genus-level *Staphylococcus* and species-level *S. capitis* and *S. warneri* abundances were higher in patients that eventually responded to phototherapy. These findings suggest commensal staphylococci abundance could help prognosticate disease responsiveness to phototherapy. Patient heterogeneity may limit the applicability of this theory, which warrants further study. Moreover, fewer significant differences were found between the species-level *Staphylococcus* profiles of non-responders and no-nbUVB patients than responders and no-nbUVB patients. This observation could indicate that the benefit of phototherapy in CTCL may be derived from the modulation of non-*S. aureus* species. Similarly, *S. epidermidis* trended higher in R after phototherapy across lesional and non-lesional skin. While the importance of coagulase-negative staphylococci to CTCL disease activity has yet to be determined, quorum sensing – as has been discussed in AD – could explain this finding (47). Further, very recent research revealed *S. warneri* exhibits methicillin-resistant *S. aureus* quorum sensing activity that helps protect skin from atopic and necrotic damage (48). Lastly, *S. epidermidis* – a very common commensal coagulase-negative staphylococcal species – contributes to skin microbial homeostasis through its ability to inhibit *S. aureus* growth *via* the production of antimicrobial peptides (49) and interfering with *S. aureus* biofilm production (50). Additionally, *S. epidermidis* has been shown to have anti-tumor properties in UV-induced skin cancers (51) and can suppress cutaneous inflammation by activating regulatory T-cells (52).

Other notable genera from this analysis included *Acinetobacter*, *Corynebacterium*, *Brevibacterium*, and *Streptococcus*. As *in vitro* studies have demonstrated *Acinetobacter* can induce anti-

10.3389/fimmu.2022.1022093

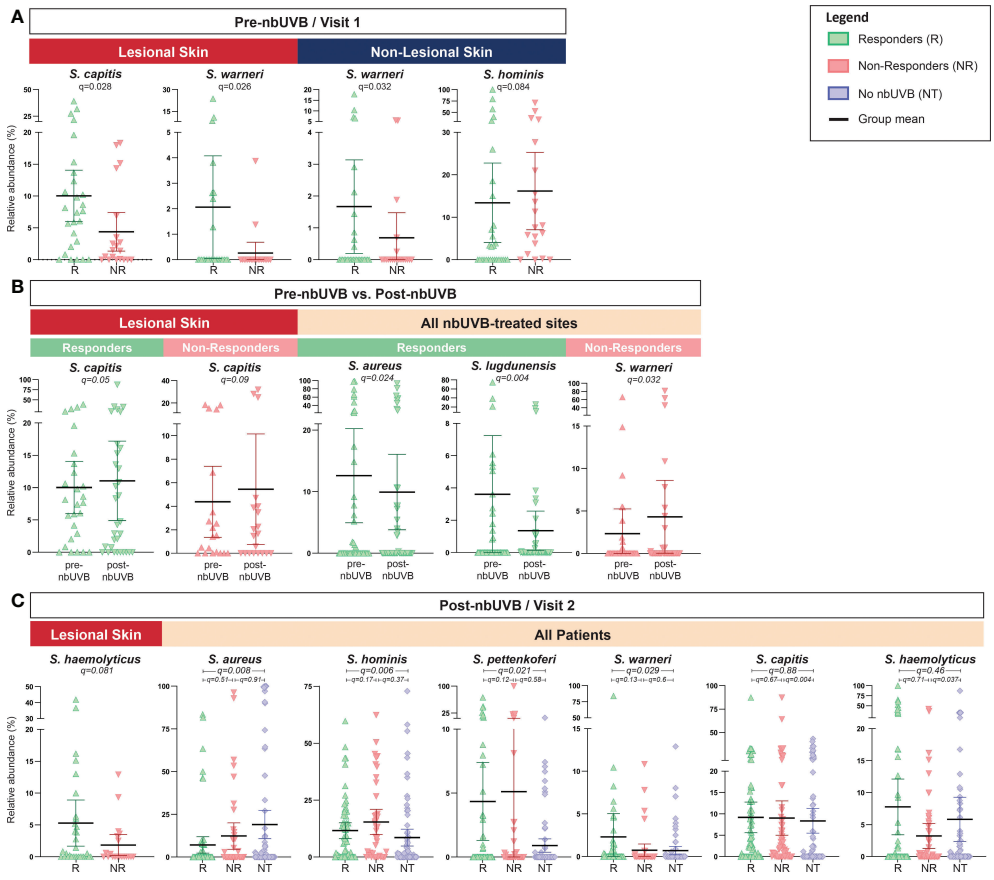

FIGURE 5
Staphylococcus species abundance differentiates nbUVB responders, nbUVB non-responders, and no-nbUVB patients. Differential analysis demonstrated significant shifts in various staphylococcal species including *S. aureus*, *S. lugdunensis*, *S. hominis*, and *S. haemolyticus* characterize R, NR, and no-nbUVB (not treated; NT) skin **(A)** pre-nbUVB, **(B)** pre- versus post-nbUVB, and **(C)** post-nbUVB. Black horizontal bars indicate group means with 95% confidence interval.

inflammatory IL-10 expression in both monocytes and keratinocytes (53), our observation that *Acinetobacter* abundance was greater in responder than non-responder lesional skin after phototherapy suggests direct linkages exist between skin microbiota and the local inflammatory microenvironment in CTCL. Moreover, little is known about the effect of nbUVB on skin microbiota. Increased abundance of healthy skin commensal flora (e.g., *Anaerococcus*, *Streptococcus*, and *Acinetobacter*) in lesional skin after phototherapy may reflect the reconstitution of a balanced skin microbiome. Increased *Streptococcus* abundance has been associated with successful treatment of AD and recovery of disease-related skin dysbiosis (54). Our data also mirrored previous research demonstrating nbUVB treatment is associated with increased *Corynebacterium* abundance (11). In addition to its potent anti-staphylococcal powers (55), this genus may influence CTCL skin activity depending on disease stage. As *Corynebacterium*-induced skin inflammation is contextually influenced by the host's overall metabolic state and gut dysbiosis severity is tied to more advanced CTCL, further study of the *gut-skin* axis and *Corynebacterium* in CTCL is warranted (19, 56). Our findings clearly demonstrated a deep and unexplored network of ASVs arising from *Corynebacterium* genera, each with specific responses among the research interrogations performed longitudinally here. This strongly suggests that there is an as-yet unexplored diversity of responses to clinically-relevant interventions that manifest as changes at the sub-genus level.

Ours is the largest evaluation of the skin microbiota in CTCL to date and the first to evaluate the impact of a therapy on this microcosm within CTCL. The novel identification of genus-level shifts in the microbiome of non-lesional skin introduces the idea that the microbial profiles of these sites could be utilized to anticipate nbUVB responsiveness. While our study is limited by the heterogeneity and distribution of disease stage within our cohort, capturing the larger shifts in the microbiome across disease stage in CTCL has yet to be thoroughly documented. Just as transcriptional heterogeneity has been associated with CTCL

(57), we expect the influence of the microbiome may vary on both inter- and intra-patient bases. Larger datasets may provide greater statistical power for conducting multivariate analyses. Furthermore, the likelihood that multiple bacterial species influence CTCL substantiate why shifts in some genera were identified in our cohort while others (e.g., *Bacillus*) were not found in our samples, despite their potential connection to CTCL tumorigenesis (24). Future analysis accounting for geographical variations in human microbiota composition is also warranted (58).

Microbes contribute to the impaired skin barrier integrity and altered local immune activity known of CTCL (59) and the extent of skin dysbiosis has been associated with disease stage (22). Here, we establish that the skin microbiome could also involve microbial biomarkers that predict nbUVB response, such as greater *Staphylococcus* relative abundance, yet we also recognize that patient heterogeneity will require further assessment in this research area. Larger and ideally multicenter analyses will validate these observations and expand upon their clinical translation.

Data availability statement

The datasets presented in this study can be found in online repositories. The names of the repository/repositories and accession number(s) can be found below: https://www.ncbi.nlm.nih.gov/bioproject/PRJNA853302.

Ethics statement

The studies involving human participants were reviewed and approved by the Northwestern University Institutional Review Board (STU00209226). The patients/participants provided their written informed consent to participate in this study.

Author contributions

Conceptualization: XZ; Data Curation: XZ, TL, MH, and FV; Formal Analysis: GE, MB, DS, and SG; Funding Acquisition: XZ; Investigation: XZ, TL, MH, and FV; Methodology: SG, XZ, and PS; Project administration: XZ and JG; Resources: XZ, JG, SG, and MB; Software: MB and SG; Supervision: XZ, PS, and JG; Validation: XZ, MB, and SG; Visualization: MH and GE; Writing – original draft: MH and XZ; Writing – review and editing: MH, XZ, JG, MB, JC, SG, GE, FV, and TL. All authors contributed to the article and approved the submitted version.

Funding

Supported by a Dermatology Foundation Medical Dermatology Career Development Award, Cutaneous Lymphoma Foundation Catalyst Research Grant, American Cancer Society Institutional Research Grant, and an institutional grant from the Northwestern University Clinical and Translational Sciences Institute (NUCATS) and the National Institutes of Health (NIH) (GRANT KL2TR001424).

Acknowledgments

The authors would like to thank the patients who contributed to the study.

Conflict of interest

The authors declare that the research was conducted in the absence of any commercial or financial relationships that could be construed as a potential conflict of interest.

Publisher's note

Supplementary material

The Supplementary Material for this article can be found online at: https://www.frontiersin.org/articles/10.3389/fimmu.2022.1022093/full#supplementary-material

References

1. Willerslev-Olsen A, Krejsgaard T, Lindahl LM, Bonefeld CM, Wasik MA, Koralov SB, et al. Bacterial toxins fuel disease progression in cutaneous T-cell lymphoma. *Toxins* (2013) 5(8):1402–21. doi: 10.3390/toxins5081402

2. Blümel E, Willerslev-Olsen A, Gluud M, Lindahl LM, Fredholm S, Nastasi C, et al. Staphylococcal alpha-toxin tilts the balance between malignant and non-malignant Cd4(+) T cells in cutaneous T-cell lymphoma. *Oncoimmunology* (2019) 8(11):e1641387–e. doi: 10.1080/2162402X.2019.1641387

3. Blümel E, Munir Ahmad S, Nastasi C, Willerslev-Olsen A, Gluud M, Fredholm S, et al. Staphylococcus aureus alpha-toxin inhibits Cd8+ T cell-mediated killing of cancer cells in cutaneous T-cell lymphoma.

Oncoimmunology (2020) 9(1):1751561. doi: 10.1080/2162402X.2020.1751561

4. Lindahl LM, Willerslev-Olsen A, Gjerdrum LMR, Nielsen PR, Blümel E, Rittig AH, et al. Antibiotics inhibit tumor and disease activity in cutaneous T-cell lymphoma. *Blood* (2019) 134(13):1072–83. doi: 10.1182/blood.2018888107

5. Axelrod PI, Lorber B, Vonderheid EC. Infections complicating mycosis fungoides and sézary syndrome. *JAMA J Am Med Assoc* (1992) 267(10):1354–8. doi: 10.1001/jama.1992.03480100060031

6. Patra V, Laoubi L, Nicolas J-F, Vocanson M, Wolf P. A perspective on the interplay of ultraviolet-radiation, skin microbiome and skin resident memory tcrαβ+ cells. *Front Med* (2018) 5:166. doi: 10.3389/fmed.2018.00166

7. Silva SH, Guedes ACM, Gontijo B, Ramos AMC, Carmo LS, Farias LM, et al. Influence of narrow-band uvb phototherapy on cutaneous microbiota of children with atopic dermatitis. *J Eur Acad Dermatol Venereology* (2006) 20(9):1114–20. doi: 10.1111/j.1468-3083.2006.01748.x

8. Mukherjee S, Mitra R, Maitra A, Gupta S, Kumaran S, Chakrabortty A, et al. Sebum and hydration levels in specific regions of human face significantly predict the nature and diversity of facial skin microbiome. *Sci Rep* (2016) 6(1):36062. doi: 10.1038/srep36062

9. Chen YE, Fischbach MA, Belkaid Y. Skin microbiota–host interactions. *Nature* (2018) 553(7689):427–36. doi: 10.1038/nature25177

10. Kurosaki Y, Tsurumachi M, Kamata Y, Tominaga M, Suga Y, Takamori K. Effects of 308 nm excimer light treatment on the skin microbiome of atopic dermatitis patients. *Photodermatology photoimmunology photomedicine* (2020) 36(3):185–91. doi: 10.1111/phpp.12531

11. Kwon S, Choi JY, Shin J-W, Huh C-H, Park K-C, Du M-H, et al. Changes in lesional and non-lesional skin microbiome during treatment of atopic dermatitis. *Acta dermato-venereologica* (2018) 99(3):284–90. doi: 10.2340/00015555-3089

12. Wang W-M, Jin H-Z. Skin Microbiome: An actor in the pathogenesis of psoriasis. *Chin Med J* (2018) 131(1):95–8. doi: 10.4103/0366-6999.221269

13. Liang X, Ou C, Zhuang J, Li J, Zhang F, Zhong Y, et al. Interplay between skin microbiota dysbiosis and the host immune system in psoriasis: Potential pathogenesis. *Front Immunol* (2021) 12:764384. doi: 10.3389/fimmu.2021.764384

14. Lam SY, Radjabzadeh D, Eppinga H, Nossent YRA, van der Zee HH, Kraaij R, et al. A microbiome study to explore the gut-skin axis in hidradenitis suppurativa. *J Dermatol Sci* (2021) 101(3):218–20. doi: 10.1016/j.jdermsci.2020.12.008

15. McCarthy S, Barrett M, Kirthi S, Pellanda P, Vlckova K, Tobin AM, et al. Altered skin and gut microbiome in hidradenitis suppurativa. *J Invest Dermatol* (2022) 142(2):459–68.e15. doi: 10.1016/j.jid.2021.05.036

16. Yuan X, Wang L, Meng D, Wu L, Wang X, Zhang D, et al. The impact of nbuvb on microbial community profiling in the lesional skin of vitiligo subjects. *Microbial pathogenesis* (2020) 140:103943–. doi: 10.1016/j.micpath.2019.103943

17. Bzioueche H, Simonyté Sjödin K, West CE, Khemis A, Rocchi S, Passeron T, et al. Analysis of matched skin and gut microbiome of patients with vitiligo reveals deep skin dysbiosis: Link with mitochondrial and immune changes. *J Invest Dermatol* (2021) 141(9):2280–90. doi: 10.1016/j.jid.2021.01.036

18. Olesen CM, Ingham AC, Thomsen SF, Clausen ML, Andersen PS, Edslev SM, et al. Changes in skin and nasal microbiome and staphylococcal species following treatment of atopic dermatitis with dupilumab. *Microorganisms* (2021) 9(7):1487. doi: 10.3390/microorganisms9071487

19. Hooper MJ, LeWitt TM, Pang Y, Veon FL, Chlipala GE, Feferman L, et al. Gut dysbiosis in cutaneous T-cell lymphoma is characterized by shifts in relative abundances of specific bacterial taxa and decreased diversity in more advanced disease. *J Eur Acad Dermatol Venereology* (2022) 36(9):1552–63. doi: 10.1111/jdv.18125

20. Hooper MJ, LeWitt TM, Veon FL, Pang Y, Chlipala GE, Feferman L, et al. Nasal dysbiosis in cutaneous T-cell lymphoma is characterized by shifts in relative abundances of non-staphylococcus bacteria. *JID Innovations* (2022) 2(5):100132. doi: 10.1016/j.xjidi.2022.100132

21. Harkins CP, MacGibeny MA, Thompson K, Bubic B, Huang X, Brown I, et al. Cutaneous T-cell lymphoma skin microbiome is characterized by shifts in certain commensal bacteria but not viruses when compared with healthy controls. *J Invest Dermatol* (2021) 141(6):1604–8. doi: 10.1016/j.jid.2020.10.021

22. Salava A, Deptula P, Lyyski A, Laine P, Paulin L, Väkevä L, et al. Skin microbiome in cutaneous T-cell lymphoma by 16s and whole-genome shotgun sequencing. *J Invest Dermatol* (2020) 140(11):2304–8.e7. doi: 10.1016/j.jid.2020.03.951

23. Zhang Y, Seminario-Vidal L, Cohen L, Hussaini M, Yao J, Rutenberg D, et al. Tcl-036: Alternations in the skin microbiota are associated with symptom severity in mycosis fungoides. *Clin lymphoma myeloma leukemia* (2021) 21:S409–S. doi: 10.1016/S2152-2650(21)01922-4

24. Dehner CA, Ruff WE, Greiling T, Pereira MS, Redanz S, McNiff J, et al. Malignant T cell activation by a bacillus species isolated from cutaneous T-cell lymphoma lesions. *JID Innov* (2022) 2(2):100084. doi: 10.1016/j.xjidi.2021.100084

25. Jost M, Wehkamp U. The skin microbiome and influencing elements in cutaneous T-cell lymphomas. *Cancers* (2022) 14(5):1324. doi: 10.3390/cancers14051324

26. Phan K, Ramachandran V, Fassihi H, Sebaratnam DF. Comparison of narrowband uv-b with psoralen–uv-a phototherapy for patients with early-stage mycosis fungoides: A systematic review and meta-analysis. *JAMA Dermatol* (2019) 155(3):335–41. doi: 10.1001/jamadermatol.2018.5204

27. Yoshimura-Mishima M, Akamatsu H, Namura S, Horio T. Suppressive effect of ultraviolet (Uvb and puva) radiation on superantigen production by staphylococcus aureus. *J Dermatol Sci* (1999) 19(1):31–6. doi: 10.1016/S0923-1811(98)00046-2

28. Naqib A, Poggi S, Wang W, Hyde M, Kunstman K, Green SJ. Making and sequencing heavily multiplexed, high-throughput 16s ribosomal rna gene amplicon libraries using a flexible, two-stage pcr protocol. *Gene Expression Anal* (2018) 1783:149–69. doi: 10.1007/978-1-4939-7834-2_7

29. Walters W, Hyde ER, Berg-Lyons D, Ackermann G, Humphrey G, Parada A, et al. Improved bacterial 16s rrna gene (V4 and V4-5) and fungal internal transcribed spacer marker gene primers for microbial community surveys. *mSystems* (2016) 1(1):e00009-15. doi: 10.1128/mSystems.00009-15

30. Prakash O, Green S, Jasrotia P, Overholt W, Canion A, Watson DB, et al. Description of rhodanobacter denitrificans sp. nov., isolated from nitrate-rich zones of a contaminated aquifer. *Int J systematic evolutionary Microbiol* (2012) 62(10):2457–62. doi: 10.1099/ijs.0.035840-0

31. Martin M. Cutadapt removes adapter sequences from high-throughput sequencing reads. *EMBnet.journal* (2011) 17(1):3. doi: 10.14806/ej.17.1.200

32. Callahan BJ, McMurdie PJ, Rosen MJ, Han AW, Johnson AJA, Holmes SP. Dada2: High-resolution sample inference from illumina amplicon data. *Nat Methods* (2016) 13(7):581–3. doi: 10.1038/nmeth.3869

33. Quast C, Pruesse E, Yilmaz P, Gerken J, Schweer T, Yarza P, et al. The Silva ribosomal rna gene database project: Improved data processing and web-based tools. *Nucleic Acids Res* (2012) 41(D1):D590–D6. doi: 10.1093/nar/gks1219

34. Murali A, Bhargava A, Wright ES. Idtaxa: A novel approach for accurate taxonomic classification of microbiome sequences. *Microbiome* (2018) 6(1):140. doi: 10.1186/s40168-018-0521-5

35. Davis NM, Proctor DM, Holmes SP, Relman DA, Callahan BJ. Simple statistical identification and removal of contaminant sequences in marker-gene and metagenomics data. *Microbiome* (2018) 6(1):226. doi: 10.1186/s40168-018-0605-2

36. Ahle CM, Stødkilde K, Afshar M, Poehlein A, Ogilvie LA, Söderquist B, et al. Staphylococcus saccharolyticus: An overlooked human skin colonizer. *Microorganisms* (2020) 8(8):1105. doi: 10.3390/microorganisms8081105

37. Ahle CM, Stødkilde-Jørgensen K, Poehlein A, Streit WR, Hüpeden J, Brüggemann H. Comparison of three amplicon sequencing approaches to determine staphylococcal populations on human skin. *BMC Microbiol* (2021) 21(1):221. doi: 10.1186/s12866-021-02284-1

38. McMurdie PJ, Holmes S. Phyloseq: An r package for reproducible interactive analysis and graphics of microbiome census data. *PLoS One* (2013) 8(4):e61217. doi: 10.1371/journal.pone.0061217

39. R Core Team.. R: A language and environment for statistical computing. Vienna, Austria: Vienna, Austria (2022). Available at: https://ww.R-project.org.

40. Okansen J, Guillaume Blanchet F, Kindt R, Legendre P, Minchin P, O'Hara R, et al. Vegan: Community ecology. *R Package Version* (2018) 2:4–6. Avalibale at: https://github.com/vegandevs/vegan.

41. Kuhn M. The caret package. *J Stat Software* (2012) 28(5):1–26. doi 10.18637/jss.v028.i05.

42. Ho TK. (1995). Random decision forests, in: *Proceedings of the Third International Conference on Document Analysis and Recognition*, Montreal, (14-16) 278–82.

43. Robin X, Turck N, Hainard A, Tiberti N, Lisacek F, Sanchez J-C, et al. Proc: An open-source package for r and s+ to analyze and compare roc curves. *BMC Bioinf* (2011) 12(1):77. doi: 10.1186/1471-2105-12-77

44. Paulson JN, Stine OC, Bravo HC, Pop M. Differential abundance analysis for microbial marker-gene surveys. *Nat Methods* (2013) 10(12):1200–2. doi: 10.1038/nmeth.2658

45. Robinson MD, McCarthy DJ, Smyth GK. Edger: A bioconductor package for differential expression analysis of digital gene expression data. *Bioinformatics* (2010) 26(1):139–40. doi: 10.1093/bioinformatics/btp616

46. Krejsgaard T, Willerslev-Olsen A, Lindahl LM, Bonefeld CM, Koralov SB, Geisler C, et al. Staphylococcal enterotoxins stimulate lymphoma-associated immune dysregulation. *Blood* (2014) 124(5):761–70. doi: 10.1182/blood-2014-01-551184

47. Williams MR, Costa SK, Zaramela LS, Khalil S, Todd DA, Winter HL, et al. Quorum sensing between bacterial species on the skin protects against epidermal

injury in atopic dermatitis. *Sci Transl Med* (2019) 11(490):eaat8329. doi: 10.1126/scitranslmed.aat8329

48. Severn MM, Cho YK, Manzer HS, Bunch ZL, Shahbandi A, Todd DA, et al. The commensal staphylococcus warneri makes peptide inhibitors of mrsa quorum sensing that protect skin from atopic or necrotic damage. *J Invest Dermatol* (2022) S0022-202X(22)01646-3. doi: 10.1016/j.jid.2022.05.1092

49. Nakatsuji T, Chen TH, Narala S, Chun KA, Two AM, Yun T, et al. Antimicrobials from human skin commensal bacteria protect against staphylococcus aureus and are deficient in atopic dermatitis. *Sci Transl Med* (2017) 9(378):eaah4680. doi: 10.1126/scitranslmed.aah4680

50. Glatthardt T, Campos JCM, Chamon RC, de Sá Coimbra TF, Rocha GA, de Melo MAF, et al. Small molecules produced by commensal staphylococcus epidermidis disrupt formation of biofilms by staphylococcus aureus. *Appl Environ Microbiol* (2020) 86(5):e02539-19. doi: 10.1128/aem.02539-19

51. Nakatsuji T, Chen TH, Butcher AM, Trzoss LL, Nam SJ, Shirakawa KT, et al. A commensal strain of staphylococcus epidermidis protects against skin neoplasia. *Sci Adv* (2018) 4(2):eaao4502. doi: 10.1126/sciadv.aao4502

52. Laborel-Préneron E, Bianchi P, Boralevi F, Lehours P, Fraysse F, Morice-Picard F, et al. Effects of the staphylococcus aureus and staphylococcus epidermidis secretomes isolated from the skin microbiota of atopic children on Cd4+ T cell activation. *PLoS One* (2015) 10(10):e0141067–e. doi: 10.1371/journal.pone.0141067

53. Fyhrquist N, Ruokolainen L, Suomalainen A, Lehtimäki S, Veckman V, Vendelin J, et al. Acinetobacter species in the skin microbiota protect against allergic sensitization and inflammation. *J Allergy Clin Immunol* (2014) 134 (6):1301–9.e11. doi: 10.1016/j.jaci.2014.07.059

54. Kong HH, Oh J, Deming C, Conlan S, Grice EA, Beatson MA, et al. Temporal shifts in the skin microbiome associated with disease flares and treatment in children with atopic dermatitis. *Genome Res* (2012) 22(5):850–9. doi: 10.1101/gr.131029.111

55. Flowers L, Grice EA. The skin microbiota: Balancing risk and reward. *Cell Host Microbe* (2020) 28(2):190–200. doi: 10.1016/j.chom.2020.06.017

56. Ridaura VK, Bouladoux N, Claesen J, Chen YE, Byrd AL, Constantinides MG, et al. Contextual control of skin immunity and inflammation by corynebacterium. *J Exp Med* (2018) 215(3):785–99. doi: 10.1084/jem.20171079

57. Licht P, Mailänder V. Transcriptional heterogeneity and the microbiome of cutaneous T-cell lymphoma. *Cells* (2022) 11(3):328. doi: 10.3390/cells11030328

58. Gupta VK, Paul S, Dutta C. Geography, ethnicity or subsistence-specific variations in human microbiome composition and diversity. *Front Microbiol* (2017) 8:1162. doi: 10.3389/fmicb.2017.01162

59. Suga H, Sugaya M, Miyagaki T, Ohmatsu H, Kawaguchi M, Takahashi N, et al. Skin barrier dysfunction and low antimicrobial peptide expression in cutaneous T-cell lymphoma. *Clin Cancer Res* (2014) 20(16):4339–48. doi: 10.1158/1078-0432.Ccr-14-0077